ELSEVIER

Catalysis Today 63 (2000) 309–315

CATALYSIS TODAY

www.elsevier.com/locate/cattod

Evidence of furan formation from acetaldehyde over β-UO_3

H. Madhavaram, H. Idriss*

Materials Chemistry, Department of Chemistry, The University of Auckland, Private Bag 92019, Auckland, New Zealand

Abstract

Furan, C_4H_4O, has been observed from acetaldehyde over β-UO_3 during temperature programmed desorption (TPD) with a high yield (ca. 40%) at low surface coverage. At high surface coverage crotonaldehyde, $CH_3CH{=}CHCHO$ (formed by β-aldolisation of acetaldehyde), was the most dominant product. Flow experiments at $P = 30$ atm have indicated that one can achieve high reaction selectivity to furan. The catalyst deactivated, however, after a few hours of time on stream. X-ray diffraction analyses have shown that β-UO_3 has been reduced to a mixture of α-U_3O_8 and UO_2. The catalysts could be regenerated by gas-phase O_2 at 673–773 K, 30–40 atm for 2 h. The comparison between furan formation from acetaldehyde to that from ethylene as well as from ethanol [J. Catal. 184 (1999) 553; Stud. Surf. Sci. Catal. 110 (1997) 265] over U oxides indicates the following. (1) β-UO_3 was far more active than α-U_3O_8. (2) Acetaldehyde gave the highest reaction yield. (3) The reaction appears to be driven by the high oxidation state of U cations (U^{+6}) as well as the potential presence of these U^{+6} cations in a sixfold coordination environment, i.e. containing two vacancies to accommodate the coupling of two C2 molecules to the C4 furan product. © 2000 Elsevier Science B.V. All rights reserved.

Keywords: Furan; TPD; X-ray diffraction; Acetaldehyde

1. Introduction

Uranium oxides have been used as heterogeneous catalysts, promoters, as well as supports for other catalysts in various reactions of industrial importance involving natural gas or coal based fuels, and petroleum and organic products [1]. The general formula for uranium oxides, U_nO_{2n+2}, accounts for a number, but not all of the reported oxides. Uranium can assume at least three main valencies. +2 (UO), +4 (UO_2), and +6 (UO_3) in the solid state [1]. The binary oxides (in order of increasing O/U ratios) that have been reported at one time or another are: UO, UO_2, U_4O_9, $U_{16}O_{37}$, U_3O_7, U_2O_5, U_5O_{13}, $U_{13}O_{34}$, U_8O_{21}, $U_{11}O_{29}$, U_3O_8, $U_{12}O_{35}$ and UO_3 [2]. Stimulated in a large part by their potential use as nuclear fuels, large areas of the complicated uranium oxide phase diagram have been studied, revealing many mixed valance materials like U_3O_8 and U_4O_9.

UO_2 is an active and stable catalyst for the dehydrogenation of ethyl benzene to styrene and cumene to α-methyl styrene [3]. It is also active for the dehydration/dehydrogenation of ethanol [4] and dehydration of acetic acid [5]. U_3O_8 has exceedingly high oxidative activity in the catalytic oxidation of carbon monoxide, far higher than that of V_2O_5, MoO_3, or WO_3 [6]. It is also active for the complete destruction of environmentally undesirable volatile organic compounds (VOCs) like chlorobenzene, benzene, butane, cyclohexanone and butyl acetate [7,8]. In addition, the presence of alkali and alkaline earth elements on U_3O_8 increases its activity for the oxidation of CO by NO [9]. Moreover, it has been shown that if uranium is correctly impregnated, it can strongly improve the

---

* Corresponding author. Tel.: +64-9-3737599;
fax: +64-9-3737422.
E-mail address: h.idriss@auckland.ac.nz (H. Idriss).

PII: S0920-5861(00)00474-0

Table 1
The different phases of UO_3

Type	Structure
UO_3 amorphous	[12]
α-UO_3	Hexagonal [29], Orthorhombic [30]
β-UO_3	Monoclinic [13]
γ-UO_3	Orthorhombic [31], Tetragonal [32]
δ-UO_3	Cubic [33]
ζ-UO_3	Hexagonal [34]
η-UO_3	Orthorhombic [35]
ε-UO_3	Monoclinic [36]

dispersion quality of alumina [10]. It was also reported that addition of uranium (in the +4 oxidation state) specifically improves the activity of SiC as a catalyst support for CoMo catalysts for hydrodesulphurisation (HDS) of thiophen [10]. Moreover, Bismuth–uranium catalysts are active for the oxidative demethylation of toluene [3] as well as for the formation of acrylonitrile and acrolein by ammoxidation and oxidation of propylene, respectively [11].

UO_3 is considered the principal species in the gas phase of uranium oxides. One amorphous and 7 crystalline modifications of UO_3 are known. α-, β-, δ-, ε-, γ-, ζ- and η-UO_3 [12]. One may obtain different phases of UO_3 by changing the preparation conditions of the decomposition of the starting materials. For example, uranyl nitrate calcined rapidly at 773 K for 3–4 h results in the formation of β-UO_3, while calcination at 3°C/min to 773 K yields γ-UO_3 [13]. The colour of the respective phases depends upon the method of preparation. For example, the β-phase prepared from ammonium uranate or uranium nitrate is dark orange, while that prepared by U_3O_8 oxidation product is a cherry red [14]. Table 1 presents the different phases of UO_3.

We have previously shown that U oxides are also active for C-C bond formation reactions. Acetone was converted to isobutene on α-U_3O_8 [15] (isobutene has been observed from acetone by other workers over CeO_2 [16] and Gd_2O_3 [17]) and mainly dehydrated to propene on UO_2. These results indicated a structure-sensitive nature and/or or a sensitivity to the oxidation state of U cations (U_3O_8 is composed of U^{+6} and U^{+4} cations) [15]. Moreover, we have also reported the formation of furan from ethanol as well as from ethylene in a single step stoichiometric reaction over β-UO_3 [18,19].

Furan and furan derivatives are raw materials for the production of industrial chemicals for use as pharmaceuticals, herbicides, stabilisers. They are also building blocks for conducting polymers, which are used for device fabrics and anticorrosion coating applications for inorganic semiconductors [20], and in the production of tetrahydrofuran by hydrogenation [21]. However, the classical methods of furan production are very expensive. In fact, the challenge is the production of furan in a one-step gas-phase reaction using C4 hydrocarbon feedstock, which would be an attractive alternative to currently applied multistage process [22]. It is commercially prepared by: the decarbonylation of furfural over catalysts based on nickel or cobalt or by pyrolysis at 700°C [23], oxidation of butadiene over molybdenum–bismuth catalyst [24], or hydrogenation of maleic anhydride [25]. This work presents the catalytic formation of furan from acetaldehyde over β-UO_3 catalyst by temperature programmed desorption (TPD) and catalytic tests and shows that one can obtain furan from acetaldehyde in a high yield.

2. Experimental

β-UO_3 was prepared from uranium nitrate solution. $U(OH)_6$ was precipitated with ammonia solution at pH 9. The precipitate was filtered and washed in water. The filtered precipitate was dried at 373 K overnight and calcined at 773 K for 18 h [13]. XRD (Fig. 1) indicated a pure form of β-UO_3 and confirmed the absence of any other uranium oxide phases. Several UO_3 preparations have been performed. In most of the cases a mixture of β-UO_3 and γ-UO_3 was observed with β-UO_3 as the dominant phase depending on the temperature ramping rate.

TPD was performed using a fixed-bed reactor interfaced to a high vacuum chamber equipped with a quadruple mass spectrometer (base pressure ca. 5×10^{-8} Torr, working pressure during TPD $= 2\text{–}3 \times 10^{-6}$). The reactor pressure during TPD was ca. 10^{-3} Torr at a pumping speed of ca. 10 m^3/h. The mass spectrometer is multiplexed with an IBM PC that is equipped with a program that allows the monitoring of 12 masses simultaneously at a cycling rate of ca. 2 s. The ramping rate during TPD was kept fixed at 15 K/min. The fragmentation patterns of each product were checked in order to identify unambigu-

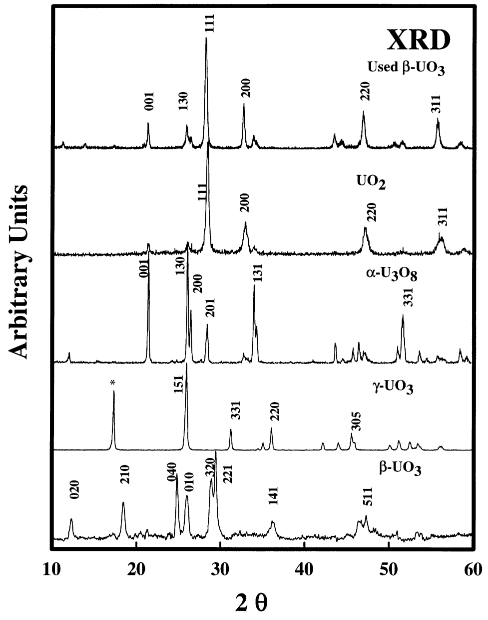

Fig. 1. X-ray diffraction of as prepared, used and regenerated U oxides. UO_2 was prepared by H_2-reduction of U_3O_8 at 773 K for 12 h; $*$ 2θ at 17.29. This value may correspond to either the (1 0 0) of UO_2 $(OH)_2$, $2\theta = 17.27$ or to the (0 0 1) of ε-$UO_3{\cdot}H_2O$, $2\theta = 17.32$.

ously the reaction products by the method described previously [26]. Mass spectrometer correction factors with respect to *m*/*e* 28 were calculated following the method described in Ref. [27].

Steady-state reactions were carried out in a fixed-bed reactor at different pressures. The reactor was placed in a programmable oven connected to a gas chromatograph (GC), equipped with flame ionisation detector (FID), via a six-way valve. To separate the products, the column (Chromosorb 102) was temperature programmed with an initial temperature of 333 K for 2 min, then ramped at 1 K/min to 393 K. The GC was coupled to a PC running PEAKSIMPLE III software for data acquisition.

Batch reactions were performed in a glass reactor (32 ml volume) which was placed in an oven. The weight (230 mg) and prior treatment of the catalyst together with the reaction temperature (473 K) were kept constant for all the experiments. The prior treatment consisted of heating the catalyst to 523 K under dry air for 1 h. The reactor was evacuated after the pretreatment of the catalyst and the desired amount of acetaldehyde and 20 ml of helium were introduced at room temperature via a rubber septum. After equilibrium was obtained the temperature was adjusted to 573 K and the reaction was followed by injecting the gas samples from the reactor into the GC/MS. In order to monitor CO and CO_2 during the batch reactions a GC, operating isothermally at 300 K, equipped with a thermal conductivity detector (TCD) and a chromosorb 102 column was used.

GC/MS instrument was a Hewlett Packard 6890 gas chromatograph coupled with Hewlett Packard 5973 mass selective detector. The GC employed a Gas Pro GSC capillary column of 30 m×0.32 mm internal diameter with helium as carrier gas. The capillary column was temperature programmed with an initial temperature of 473 K for 2 min, then ramped at 20 K/min to 513 K. The mass selective detector was set to record mass spectra in a range of 10–500 AMU at predetermined rate of 3 scans/s. A split ratio of 30:1, i.e. $\frac{1}{30}$th of the sample volume injected into the GC/MS was used. A 5 ml Hamilton gas proof lockable syringe was used to inject the gas samples into the GC/MS.

Polycrystalline α-U_3O_8 was obtained from BDH chemical, while UO_2 was prepared by H_2-reduction of α-U_3O_8. UO_2 is totally inactive for furan formation (in effects it reductively couple acetaldehyde to butene [28]) and only traces of furan were observed over α-U_3O_8.

3. Results

3.1. TPD after acetaldehyde adsorption over β-UO_3

Several TPD runs at various surface exposures of acetaldehyde over β-UO_3 were conducted. Fig. 2 and Table 2 present the desorption profile during acetaldehyde (16.2×10^3 L)-TPD on β-UO_3. A complex set of desorption products were observed. Unreacted acetaldehyde (CH_3CHO, *m*/*e* 29, 44, 43) desorbed in two temperature domains, at 340 and 450–500 K. The two main products were: crotonaldehyde at 390 K ($CH_3CH{=}CHCHO$, *m*/*e* 70, 41, 39, 69), furan at 420 K (C_4H_4O, *m*/*e* 39 and 68). In addition, small amounts of butadiene at 530 K ($CH_2{=}CHCH{=}CH_2$ *m*/*e* 39 and 54) and butene at 560 K ($CH_3CH{=}CHCH_3$ *m*/*e* 39, 56 and 55) were also detected. Along with these products traces of

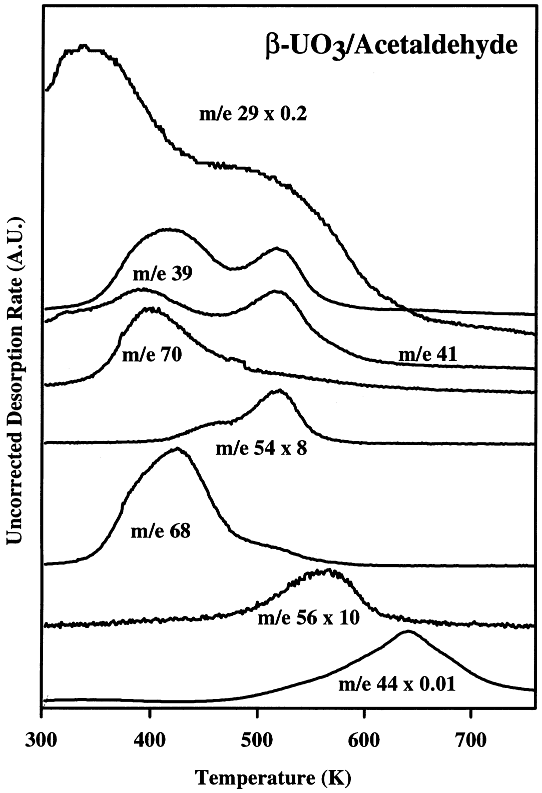

Fig. 2. TPD after acetaldehyde adsorption over β-UO_3, at room temperature.

ethanol (*m*/*e* 31, 46, 45) crotyl alcohol (*m*/*e* 72), acetone (*m*/*e* 43, 58 and 15) and crotonic acid (*m*/*e* 86, 41, 39, 69) with a combined carbon selectivity of less than 1% also desorbed. Adsorption of *m*/*e* 42 was observed at 540–550 K. Quantified analysis of the fragmentation pattern at this temperature indicated that it is most likely due to propene (*m*/*e* 41, 42 and 39) and not ketene (only traces of *m*/*e* 14 were detected). CO_2 (*m*/*e* 44) desorbed at higher temperature 700 K. Blank experiments showed comparable amounts of CO_2.

Table 2
Carbon yield and selectivity of products during TPD after acetaldehyde adsorption, over β-UO_3, at room temperature

Product	Peak temperature (K)	Carbon yield (%)	Selectivity (%)
Acetaldehyde (*m*/*e* 29)	320–340, 450–500	66	–
Furan (*m*/*e* 68)	420	10.1	30.5
Crotonaldehyde (*m*/*e*70)	390	7.2	21.6
Butene (*m*/*e* 56)	540	2.4	7.2
Butadiene (*m*/*e* 54)	560	2.1	6.4
Propene (*m*/*e* 42)	540–550	11.4	34.2

Fig. 3 presents the carbon yield obtained during several acetaldehyde-TPD runs on β-UO_3 at different initial exposures. Several points may be deduced from this figure. First, furan is highest at low coverage (reaching a carbon yield of ca. 40%), while the aldolisation reaction product, crotonaldehyde required higher surface coverage to appear. Second, no considerable change in reaction yield is observed at high exposures. This latter result may indicate that surface saturation is reached, at $\sim 3 \times 10^3$ L. Third, there were no signals corresponding to propene, butadiene or butene at low coverage.

3.2. Batch reactions

In order to study the effect of furan formation as a function of prolonged contact time, reactions of acetaldehyde on β-UO_3 were performed in a batch reactor at 473 K at different initial acetaldehyde concentrations. At high concentrations of acetaldehyde (4×10^{-6} mol/ml) along with furan other competing products appeared mainly crotonaldehyde and C4 hydrocarbons. But at lower concentrations the other reaction products decreased significantly. Fig. 4 presents furan and CO_2 formation as a function of time. The decrease of furan is concomitant with CO_2 production. In fact, 2 mol of acetaldehyde are required to make 1 mol of furan and 1 mol of acetaldehyde makes ultimately 2 mol of CO_2.

$$(O^{2-})_s + 2CH_3CHO \rightarrow C_4H_4O + 2H_2O \qquad (1)$$

$$5(O^{2-})_s + CH_3CHO \rightarrow 2CO_2 + 2H_2O \qquad (2)$$

where s is the surface. Although CO_2 production is higher than that of furan (about four times higher per mol of acetaldehyde) the high selectivity of the reaction to furan provides the required motivation for further investigations.

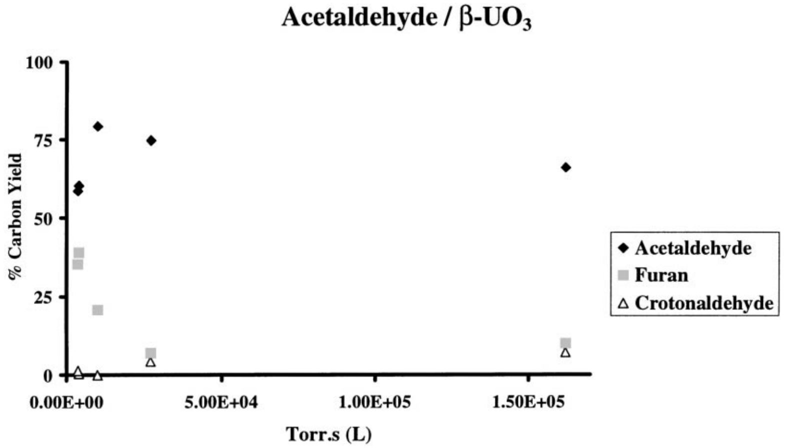

Fig. 3. Carbon yield of furan, crotonaldehyde and acetaldehyde as a function of surface coverage during TPD of acetaldehyde over β-UO_3.

3.3. Steady-state reactions

Since in order to make β-UO_3 from U_3O_8 at least 30 atm of oxygen are required, it was preferable to conduct the flow experiments at this pressure. Fig. 5 presents furan production at 30 atm and 673 K using an acetaldehyde concentration $= 2.5 \times 10^{-8}$ mol/ml, balance N_2. At these conditions, furan was the main oxygenated product detected (reaction products monitored by GC and GC–MS). Traces of benzene and C4 hydrocarbons were also observed. CO_2 was observed and basically accounted for the remaining mass balance. The catalyst was deactivated after ~5 h, however. XRD (Fig. 1) of the deactivated catalyst showed complete transformation of β-UO_3 to a mixture of

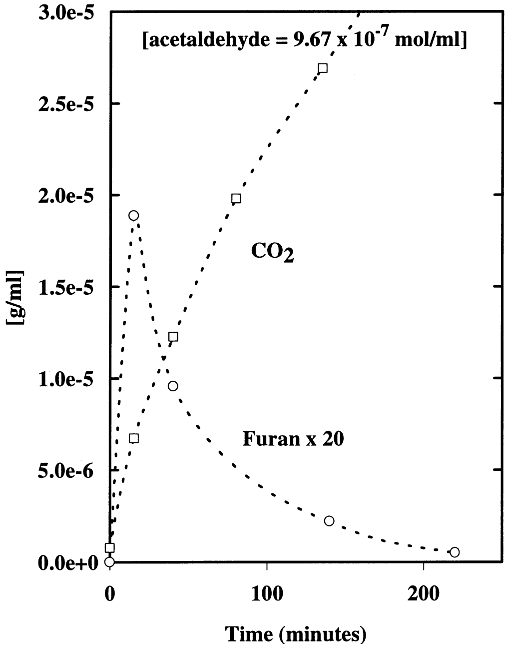

Fig. 4. Furan and CO_2 formation as a function of time over β-UO_3. Reactor volume = 32 ml, [catal.] = 230 mg, $T = 473$ K, $P = 1$ atm, $[CH_3CHO] = 9.67 \times 10^{-7}$ mol/ml.

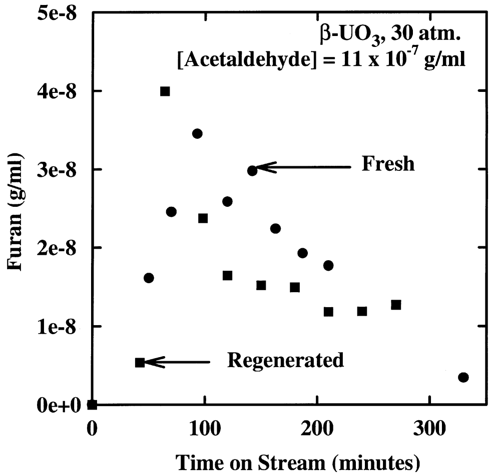

Fig. 5. Furan formation as a function of time on stream over β-UO_3. $T = 674$ K, $P = 30$ atm, $[CH_3CHO] = 2.5 \times 10^{-8}$ mol/ml (11×10^{-7} g/ml), $F/W = 25$ ml min^{-1} g catal^{-1}.

U_3O_8 and UO_2. The catalyst could however recover its catalytic activity following regeneration at 623 K for 2 h at 40 atm of O_2. Also shown in the figure the reaction of acetaldehyde on the regenerated catalyst. Clearly the regeneration has resulted in an active catalyst.

4. Discussion

In previous work we have compared the reactions of ethylene to that of ethanol for the production of furan over β-UO_3 surfaces by TPD [18,19]. As shown in the equations below acetaldehyde is far more active (on a C% basis) than ethylene or ethanol for the production of furan.

$$H_2C{=}CH_2 \Rightarrow \underset{(5\text{–}6\%)}{C_4H_4O} + CH_3CH_2OH + CH_3CHO \qquad (3)$$

$$CH_3CH_2OH \Rightarrow \underset{(20\text{–}25\%)}{C_4H_4O} + CH_3CHO \qquad (4)$$

$$CH_3CHO \Rightarrow \underset{(35\text{–}40\%)}{C_4H_4O} + \text{traces of } CH_3CH{=}CHCHO \qquad (5)$$

(the equations are not balanced for the sake of simplicity)

There are several common points in the three sets of studies (ethylene, ethanol and acetaldehyde). (1) Making furan from these appears to be driven by oxidation steps. This is based on the following observation: while acetaldehyde and ethanol are formed from ethylene no ethylene was observed from ethanol [18] and no ethanol was observed from acetaldehyde (this work). (2) Flow experiments and XRD analyses have shown that the catalyst deactivation is associated with formation of a mixture of α-U_3O_8 and UO_2 (reduction). (3) Although the formation of furan from ethylene requires oxygen transfer from the lattice that from acetaldehyde or ethanol do not necessarily require this transfer. Thus, the reduction of the substrate is associated with other side reactions. Probably the most important side reactions are the complete oxidation to CO_2 (observed but not quantified, in TPD experiments, and accounting for the remaining mass balance in flow experiments) and H_2O (observed but not quantified). Water formation is in fact related to the O to H ratio of the reactants. The lower is the ratio the more likely the reaction will proceed before total surface depletion as shown by Eqs. (1), (6) and (7)

$$2CH_2{=}CH_2 + 3(O^{2-})_s \rightarrow C_4H_4O + 2H_2O \qquad (6)$$

$$2CH_3CH_2OH + 3(O^{2-})_s \rightarrow C_4H_4O + 4H_2O \qquad (7)$$

where s is the surface.

Another important requirement is the coupling of the two C2 molecules to make furan or its precursor. We have previously [18] indicated that the presence of double vacancies is most likely the reason for the observed activity of β-$UO_{.3}$. The unit cell of β-UO_3 contains $5U^{+6}$ cations, two of them are sixfold coordinated while the remaining are sevenfold coordinated — complete coordination is with eight oxygen anions. In other words, the high oxidation state of U is necessary but not the sole factor behind furan formation. For example, while U_3O_8 contains a ratio U^{+6} to $U^{+4} = 2$ (15), all U cations are sevenfold coordinated and indeed only traces of furan are detected.

In summary, the reaction of acetaldehyde was investigated over the surfaces of β-UO_3 and α-U_3O_8. β-UO_3 was active for making furan while α-U_3O_8 was not. TPD results indicated that the selectivity to furan was high at low surface coverage while at high surface coverage the other competing reaction product, crotonaldehyde, increased considerably (Fig. 3). Flow experiments have shown that furan is the major organic product formed. Although deactivation of the catalytic material was considerable after few hours on stream the catalyst could be easily regenerated by O_2 at 30 atm and 673–773 K (Fig. 5).

Acknowledgements

HM thanks the University of Auckland for the award of a scholarship to conduct this work and HI thanks the Research Committee of the University of Auckland for grants number: 3410466 and 3410415.

References

[1] C.A. Colmenares, Prog. Solid State Chem. 9 (1974) 139.
[2] J.J. Katz, G. Seaborg, Chemistry of Lanthanides and Actinides, Vol. 1, Chapman & Hall, New York, 1986.

[3] H.W.G. Heynes, C.G.M.C. Berkel, H.S. Van Der Ban, J. Catal. 48 (1977) 386.
[4] S. Chong, T.R. Griffiths, H. Idriss, Surf. Sci. 444 (1999) 187.
[5] S. Chong, H. Idriss, J. Vac. Sci. Technol. A 18 (2000) 1900.
[6] F. Nozaki, K. Ohki, Bull. Chem. Soc. Jpn. 45 (1972) 3473.
[7] G.J. Hutchings, C.S. Heneghan, I.D. Hudson, S.H. Taylor, Nature 384 (1996) 341.
[8] C.S. Heneghan, G.J. Hutchings, S.R. O'Leary, V.J. Boyd, S.H. Taylor, I.D. Hudson, Catal. Today 54 (1999) 3.
[9] F. Nozaki, F. Matsukawa, Y. Mano, Bull. Chem. Soc. Jpn. 48 (1975) 2764.
[10] M.J. Ledoux, S. Hanter, C.P. Huu, J. Guille, M.P. Desaneaux, J. Catal. 114 (1988) 176.
[11] R.K. Grasselli, J.D. Burrington, Adv. Catal. 30 (1981) 133.
[12] M.A. Khilla, S.A. El-Fekey, N.H. Rofail, Radiochim. Acta 40 (1986) 185.
[13] P.C. Debets, Acta Cryst. 21 (1966) 589.
[14] H.R. Hoekestra, S. Siegel, J. Inorg. Nucl. Chem. 18 (1961) 154.
[15] H. Madhavaram, P. Buchanan, H. Idriss, J. Vac. Sci. Technol. A 15 (1997) 1685.
[16] M.I. Zaki, N.J. Sheppard, J. Catal. 80 (1983) 114.
[17] G.M.A. Hussein, J. Phys. Chem. 98 (1994) 9657.
[18] H. Madhavaram, H. Idriss, J. Catal. 184 (1999) 553.
[19] H. Madhavaram, H. Idriss, Stud. Surf. Sci. Catal. 110 (1997) 265.
[20] F.Q. Yan, M.H. Qiao, X.M. Wei, Q.P. Lui, J. Chem. Phys. 111 (1999) 8068.
[21] Kirk Othmer Encyclopedia of Chemical Technology, Vol. 11, 3rd Edition, Wiley, New York, 1982.
[22] M.O. Wildberger, T. Mallat, U. Göbel, A. Baiker, Appl. Catal. A 168 (1998) 69.
[23] W.H. Banford, M.M. Manes, US Patent 2,846,449 (1958).
[24] F.F. Farha Jr., US Patent 3,906,009 (1975).
[25] G. Centi, F. Trifiro, J. Mol. Catal. 25 (1986) 255.
[26] H. Idriss, K.S. Kim, M.A. Barteau, J. Catal. 139 (1993) 119.
[27] E.I. Ko, J.B. Benziger, R.J. Madix, J. Catal. 62 (1980) 264.
[28] H. Madhavaram, M.A. Barteau, H. Idriss, in: W.G. Ferguson, W. Gao (Eds.), Advanced Materials Development and Performance, July 1997, p. 46.
[29] W. Zachariasen, Acta Cryst. 1 (1948) 265.
[30] C.F. Greaves, Acta Cryst. B 28 (1972) 3609.
[31] B. Loopstra, et al., J. Solid State Chem. 20 (1977) 9.
[32] R. de Wolf, Engmann, Acta Cryst. 16 (1963) 993.
[33] E. Wait, J. Inorg. Nucl. Chem. 1 (1955) 309.
[34] L. Kuznetsov, A. Tsvigunov, Radiokhimiya 18 (1976) 414.
[35] S. Seigel, H. Hoekstra, Sherry, Acta Cryst. 20 (1966) 292.
[36] A. Tsvigunov, L. Kuznetsov, Radiokhimiya 18 (1976) 411.